

Combustion of RDX/AP Composite Propellants at Low Pressures

T. Kuwahara*

Nissan Motor Company, Ltd., Tokyo, Japan

and

N. Kubota†

Japan Defense Agency, Tokyo, Japan

The burning rate characteristics of RDX (cyclotrimethylene trinitramine)/AP (ammonium perchlorate) composite propellants were intermediate between the characteristics of RDX and AP composite propellants. Fine thermocouple traverses in the combustion zones revealed that the flame structure of the RDX/AP propellants consists of two types of flames: one type is the diffusion flame streams produced by the decomposed gases of the AP particles and the binder; the other type is the premixed flame produced by the decomposed gases of the RDX particles and/or the binder. Thus, the flame structure above the burning surface appeared to be very heterogeneous. The heat feedback from the gas phase to the burning surface was significantly reduced by the reduced reaction rate of the RDX premixed flame. Therefore the burning rate of the RDX/AP propellants was lower than that of the AP propellants. The burning rate of the RDX/AP propellants was also affected by the type of binder used. The effect of the binder on the physical and chemical processes of the RDX/AP propellant burning was the alteration of the burning surface structure and the alteration of the burning rate of the AP particles in the propellants.

Introduction

THE ultimate object of any combustion study of solid propellants is to deduce enough information about the combustion mechanism to be able to predict the burning rate characteristics. Extensive experimental studies of ammonium perchlorate (AP) composite propellants have been conducted and several models have been proposed in the past to describe the burning rate characteristics.¹⁻⁴ It has been reported that the addition of nitramine particles to AP propellants improves their combustion characteristics. For example, the burning rate spectrum can be enlarged by the addition of nitramines.^{5,6} However, there has been very little definitive research on the combustion of nitramine and nitramine/AP composite propellants.⁵⁻¹²

This research was carried out in order to understand the combustion mechanism of nitramine/AP propellants. The nitramine tested in this study was cyclotrimethylene trinitramine (RDX). The physical and chemical properties of RDX particles are different from those of AP particles. The combustion zones of AP propellants are heterogeneous structures of the propellants. The crystalline AP particles interact with the binder surrounding the individual AP particles and produce multiple diffusion flamelets above the burning surface.^{4,13} Thus, the particle size of the AP plays an important role on the burning rate of AP propellants.

On the other hand, the crystalline RDX particles decompose and produce a monopropellant flame above the burning surface of the propellants.⁷ RDX is stoichiometrically bal-

anced, and the adiabatic flame temperature is 3275 K. Accordingly, the combustion mechanism and the burning rate characteristics of conventional AP composite propellants are altered by the addition of RDX particles. In order to determine the roles of the RDX and AP particles in RDX/AP propellants on the burning rate characteristics, the combustion wave structures were examined using high-speed microphotographs and microthermocouples.

Experiment

Propellant Formulation

The burning rate characteristics of solid propellants are largely dependent on the physical and chemical properties of the propellant ingredients. In this study, the effects of the mixture ratio of RDX and AP, the particle sizes of RDX and AP, and the type of binder on the burning rate characteristics were examined. The binders used were hydroxyl terminated polybutadiene (HTPB) and hydroxyl terminated polyester (HTPE). To determine the effect of the binder concentration on the burning rate, binder concentrations of 20% and 14% were tested. The detailed chemical formulations are shown in Tables 1-3.

The strand burner used to measure the burning rates and the combustion wave structures was a modified version of a chimney type strand burner. It consisted of a combustion chamber connected to a vacuum pump through a large surge tank. Four quartz windows were mounted on the side of the combustion chamber. The temperature profiles through the combustion zones were measured by embedding microthermocouples in the propellant strands. The thermocouples were made with 5- μ m-diam Pt-Pt 10% Rh wires.

Burning Rate Characteristics

The burning rate characteristics of RDX/AP propellants with 20% HTPB as a binder are shown in Fig. 1. The mixture ratio of RDX/AP was 40/40, and the particle sizes of RDX and AP were varied as shown in Table 1. The burning rates of the AP propellant (Aa-55) and the RDX propellant (Rr-55) were also measured. The burning rates of the RDX/AP

Presented as Paper 82-1114 at the AIAA/SAE/ASME 18th Joint Propulsion Conference, Cleveland, Ohio, June 21-23, 1982; submitted June 25, 1982; revision received Oct. 13, 1983. Copyright © 1983 by N. Kubota. Published by the American Institute of Aeronautics and Astronautics with permission.

*Research Engineer, Aeronautical and Space Division; currently, Visiting Engineer, Third Research Center, Technical Research and Development Institute.

†Chief, Rocket Propulsion Laboratory, Third Research Center, Technical Research and Development Institute. Member AIAA.

Table 1 Compositions of AP, RDX/AP, and RDX propellants (20% HTPB binder) used in this study

Propellant	HTPB ^a	AP(F) ^b	AP(C) ^c	RDX(F) ^d	RDX(C) ^e
Aa-55	20	40	40	—	—
Ar-55	20	—	40	40	—
Ra-55	20	40	—	—	40
Rr-55	20	—	—	40	40

^aHTPB: R-45M. ^bAP(F): $d = 20 \mu\text{m}$. ^cAP(C): $d = 200 \mu\text{m}$.
^dRDX(F): $d = 5 \mu\text{m}$. ^eRDX(C): $d = 120 \mu\text{m}$.

Table 2 Compositions of AP, RDX/AP, and RDX propellants (14% HTPB binder) used in this study

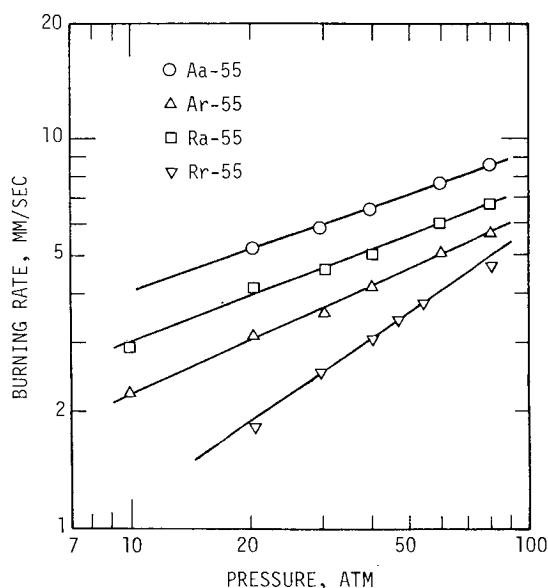
Propellant	HTPB ^a	AP(F) ^b	AP(C) ^c	RDX(F) ^d	RDX(C) ^e
PB-Aa-55	14	43	43	—	—
PB-Ar-55	14	—	43	43	—
PB-Ra-55	14	43	—	—	43
PB-Rr-55	14	—	—	43	43

^aHTPB: R-45M. ^bAP(F): $d = 20 \mu\text{m}$. ^cAP(C): $d = 200 \mu\text{m}$.
^dRDX(F): $d = 5 \mu\text{m}$. ^eRDX(C): $d = 120 \mu\text{m}$.

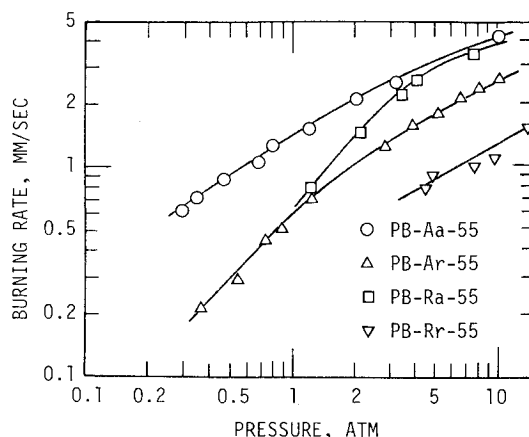
Table 3 Compositions of AP, RDX/AP, and RDX propellants (20% HTPE binder) used in this study

Propellant	HTPE ^a	AP(F) ^b	AP(C) ^c	RDX(F) ^d	RDX(C) ^e
TAa-55	20	40	40	—	—
TAr-55	20	—	40	40	—
TRa-55	20	40	—	—	40
TRr-55	20	—	—	40	40

^aHTPE: Nipporan 2200. ^bAP(F): $d = 20 \mu\text{m}$. ^cAP(C): $d = 200 \mu\text{m}$.
^dRDX(F): $d = 5 \mu\text{m}$. ^eRDX(C): $d = 120 \mu\text{m}$.

**Fig. 1** Burning rate characteristics of AP, RDX/AP, and RDX propellants (20% binder), showing decreased burning rate when RDX particles are added.

propellants (Ar-55 and Ra-55) were largely dependent on the sizes of the RDX and AP particles in the propellants. The highest burning rate was obtained with the AP propellant, and the lowest with the RDX propellant. The burning rates of RDX/AP propellants fall in the intermediate burning rate zone between the burning rates of the AP and the RDX propellants.

**Fig. 2** Burning rate characteristics of AP, RDX/AP, and RDX propellants (14% HTPB binder) at low pressures.

The pressure exponent, defined as $d \log(\text{burning rate})/d \log(\text{pressure})$ at a constant temperature, of Aa-55 was 0.34 and that of Rr-55 was 0.67. The pressure exponents of Ra-55 and Ar-55 were 0.37 and 0.44, respectively. These measurement results indicate that the burning rate of the AP propellant decreases with increasing concentration of RDX and the pressure exponent increases with increasing concentration of RDX. However, it is shown that the burning rate of the RDX propellant approaches the burning rate of the AP propellant as pressure increases.

In order to understand the combustion wave structures of RDX/AP propellants and the role of the RDX and the AP particles at the burning surface, burning rate measurements at low pressures were conducted. The overall chemical compositions of the propellants with 20% HTPB binder were fuel rich and produced a large amount of carbonaceous material on the burning surface. Therefore the measurements of the burning surface and the gas phase by microthermocouples were not possible. Thus, propellants with 14% HTPB binder instead of 20% were formulated to make the overall chemical compositions more stoichiometric. The chemical formulations of the propellants used in this study are shown in Table 2. The use of 14% HTPB binder reduced the formation of the carbonaceous material and measurements of the detailed structures of the combustion zones became possible.

The burning rate of PB-Rr-55 is an approximately straight line in a $\log(\text{pressure})$ vs $\log(\text{burning rate})$ plot (Fig. 2). However, the burning was interrupted at about 3 atm, and burning was not possible below this pressure. The burning rate was significantly increased by replacing the small-sized RDX with small-sized AP or by replacing the large-sized RDX with large-sized AP (PB-Ra-55 or PB-Ar-55). Furthermore, burning became possible even below 1 atm. The highest burning rate was obtained with PB-Aa-55.

In order to determine the effect of binder on the burning rate, propellants with 20% HTPE binder were formulated (Table 3). The burning rate characteristics of RDX/AP propellants with HTPE as a binder are shown in Fig. 3. The burning rate decreases with increasing concentration of RDX and the pressure exponent increases with increasing concentration of RDX. The overall burning rate characteristics were similar to those of the RDX/AP/HTPB propellants. However, some difference in the burning rate characteristics between RDX/AP/HTPB and RDX/AP/HTPE propellants was evident: the pressure exponent remained approximately constant for the HTPB binder in the pressure range between 10 and 80 atm. On the other hand, with the HTPE binder, the pressure exponent decreased with increasing pressure. Furthermore, with the HTPE binder, the burning interruption of TRa-55 and TRr-55 was below 10 atm, whereas the burning of TAa-55 and TAr-55 was stable at atmospheric pressure. These

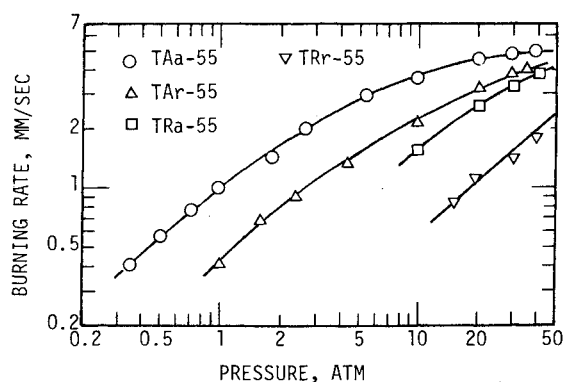


Fig. 3 Burning rate characteristics of AP, RDX/AP, and RDX propellants (20% HTPE binder) at low pressures.

results indicate that particle sizes, the mixture ratio of RDX and AP, and the type of binder cause significant effects on the burning rate characteristics of RDX/AP composite propellants.

In the following sections, the combustion wave structures of RDX/AP propellants and the roles of the RDX and AP particles in the combustion zones are determined to elucidate the burning rate characteristics of this class of propellants.

Results and Discussion

Combustion Wave Structures

The temperature profiles of the AP, RDX/AP, and RDX propellants in the combustion waves are shown in Fig. 4. The temperature gradient above the burning surface of TAa-55 was the largest for the three types of the propellants. The flame temperature of TAa-55 exceeded 1700°C, which was the upper limit of the measurement of the Pt-Pt 10% Rh thermocouples used.

The temperature in the gas phase of TRr-55 increased smoothly, reached approximately 600°C at a certain distance above the burning surface, and remained relatively constant further into the gas phase. In addition to this lowered gas phase temperature, the temperature gradient of TRr-55 was the lowest of the three types of propellants.

On the other hand, the temperature profile of TAr-55 was somewhat different from those of TAa-55 and TRr-55. The temperature of TAr-55 fluctuated in the gas phase and the amplitude of the temperature fluctuation was larger than 100°C. It was found that the observed large temperature peaks in the gas phase were produced when the AP particles in TAr-55 burned at the burning surface. The lower temperature zones between the temperature peaks were produced when the RDX particles burned at the burning surface. Thus, the flame structure of the RDX/AP propellant (TAr-55) appeared to be intermediate in nature between the flame structures of the RDX propellant (TRr-55) and the AP propellant (TAa-55).

Since the decomposition products of the AP particles react with the decomposition products of the binder and generate diffusion flame streams above the burning surface, higher temperature zones exist in the gas phase. It has been reported that RDX and the binder melt and diffuse with each other on the burning surface when HTPE binder is used.⁷ Thus, a premixed flame is generated above the burning surface. The temperature of this premixed flame is much lower than that of the AP/binder diffusion flame streams. Therefore, the flame zone of the RDX/AP propellant consists of AP/binder flames and RDX/binder flames, is highly heterogeneous, and its temperature varies largely in space and time.

In general, gas phase chemical reactions are dependent on pressure: the reaction rate decreases with decreasing pressure, and the reaction zone is enlarged in space and time. This enables measurements of the detailed structure of the reaction

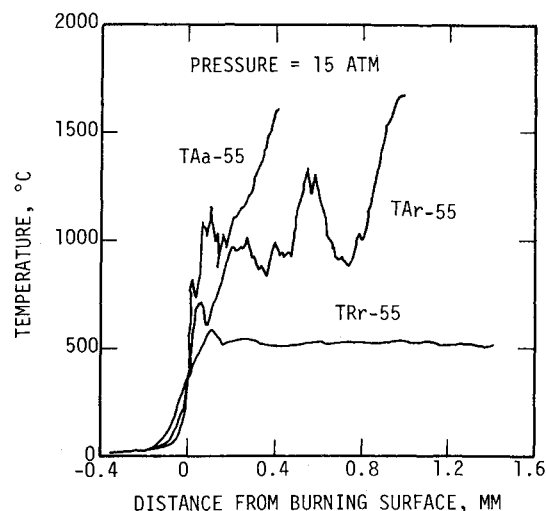


Fig. 4 Temperature profiles in the combustion zones of AP, RDX/AP, and RDX propellants (HTPE binder).

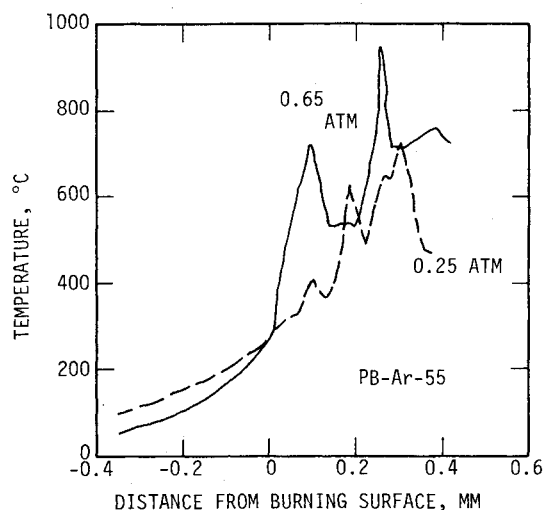


Fig. 5 Temperature profiles in the combustion zone of the RDX/AP propellant (HTPB binder) at low pressures.

zone to be done more easily. The measurements at low pressures were applied in this study in order to examine the detailed structure of the RDX/AP propellant combustion.

The temperature profiles of PB-Ar-55 at 0.65 and 0.25 atm are shown in Fig. 5. It was apparent that temperature fluctuations also existed for the RDX/AP and AP propellants. The time intervals between the temperature peaks in the fluctuated temperature profiles increased with decreasing pressure.

The temperature gradient in the gas phase just above the burning surface, $(dT/dx)_{s^+}$, was measured for the RDX/AP and AP propellants, where T is the temperature, x is the distance, and the subscript s^+ is the gas phase at the burning surface. The results are plotted logarithmically in Fig. 6. The temperature gradient for TAr-55 was much smaller than that for TAa-55. Though the measured results showed large scatter, the difference between the RDX/AP and AP propellants was evident. These results indicate that the chemical reaction in the gas phase of the RDX/AP propellant is slower than that of the AP propellant. In other words, the gas phase reaction rate of the AP propellant is delayed by the addition of RDX.

Similar results were also obtained in the case of PB-Aa-55 and PB-Ar-55, as shown in Fig. 7. However, the $(dT/dx)_{s^+}$ for PB-Aa-55 and PB-Ar-55 appeared to be more pressure sensitive than that for TAa-55 and TAr-55. In general, the burning rate of solid propellants is closely proportional to the

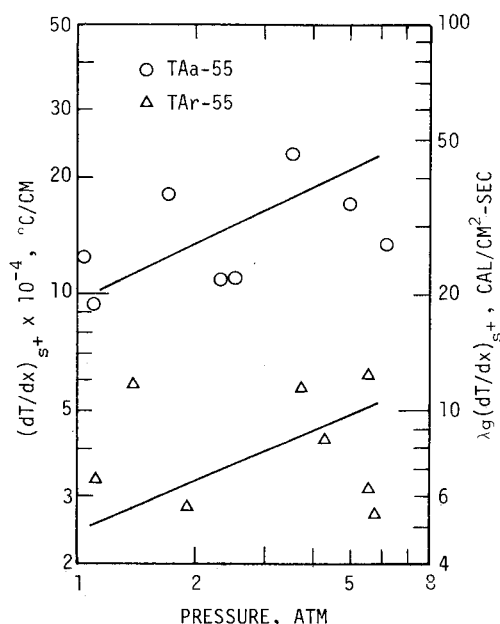


Fig. 6 Temperature gradient in the gas phase and the heat feedback from the gas phase to the burning surface of AP and RDX/AP propellants (HTPE binder).

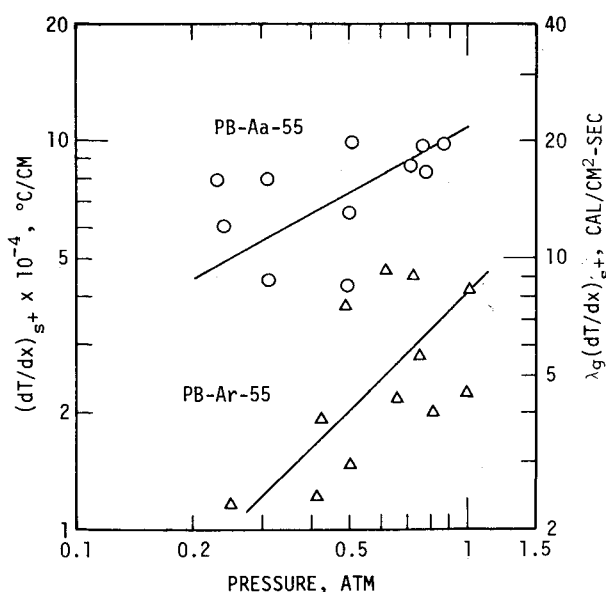


Fig. 7 Temperature gradient in the gas phase and the heat feedback from the gas phase to the burning surface of AP and RDX/AP propellants (HTPB binder).

heat feedback from the gas phase to the burning surface, q_{s+} . The q_{s+} is represented by $q_{s+} = \lambda_g (dT/dx)_{s+}$, where λ_g is the thermal conductivity of the combustion products. The calculated results of q_{s+} are shown in Fig. 6 for TAA-55 and TAR-55, and in Fig. 7 for PB-Aa-55 and PB-Ar-55. In computing the heat transfer, λ_g was assumed to be 2×10^{-4} cal/cm-s-°C. It is shown that the q_{s+} is decreased by the addition of RDX, which, in turn, decreases the burning rate. The burning rate characteristics of the AP and RDX/AP propellants tested, shown in Figs. 2 and 3, can be correlated with the results of q_{s+} shown in Figs. 6 and 7.

Determination of the Burning Rate of AP Particles in RDX/AP Propellants

It has been shown in this study that the burning rate of RDX/AP propellants is largely dependent on the burning

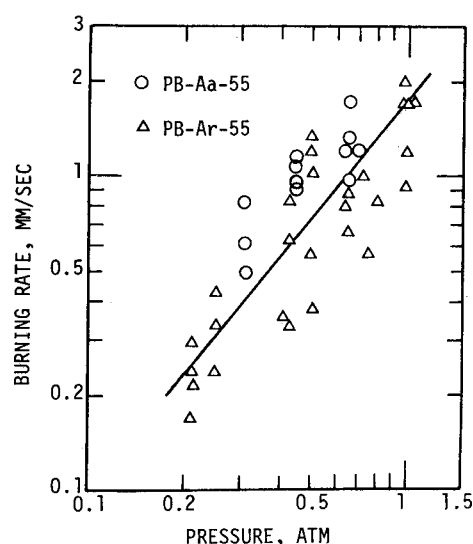


Fig. 8 Burning rate of the AP particles in AP and RDX/AP propellants (HTPB binder) showing little effect of the addition of RDX particles on burning rate.

process of the AP particles in the propellants. Experiments were carried out to determine the burning rate of the AP particles in the propellants shown in Tables 2 and 3. Since the time interval of a temperature peak shown in Figs. 4 and 5 can be assumed to be equal to the burning time of an AP particle, the burning rate of the AP particle can be determined by

$$r_{AP} = d_{AP}/\tau_{AP}$$

where r_{AP} is the burning rate of the AP particle, d_{AP} is the averaged AP particle diameter mixed in the propellant, and τ_{AP} is the time interval of the temperature peak.

The burning rates of the large-sized AP particles in PB-Aa-55 and PB-Ar-55 are shown in Fig. 8. The scatter in the data was caused possibly by the size distribution of the AP particles in the propellants and by the irregularly distributed AP/binder diffusion flame streams in the gas phase. It is evident that the burning rate of the AP particles in the RDX/AP propellant (PB-Ar-55) is approximately equal to that of the AP propellant (PB-Aa-55) in the pressure range tested. Both pressure exponents were about unity, which coincided with the pressure exponent of PB-Ar-55. The burning rate of the AP particles falls in the intermediate burning rate zone between PB-Aa-55 and PB-Ar-55. It is important to note that the burning rate of the AP particles was affected very little by the addition of the RDX particles. Since each AP particle is surrounded by binder, the burning rates of the individual AP particles are affected by the decomposition process of the binder.

In order to determine the effect of binder on the burning rate of the AP particles, the burning rate of the AP particles which were surrounded by the HTPE binder was measured.

Figure 9 shows the burning rates of the large-sized AP particles mixed in TAA-55 and TAR-55. Again, the burning rates of the AP particles were approximately the same for both propellants. The burning rates fall in the intermediate burning rate zone between the burning rates of TAA-55 and TAR-55. The pressure exponent of the r_{AP} was 0.41, which was much less than that of the r_{AP} of the propellants made with the HTPB binder. Furthermore, the pressure exponent of the r_{AP} was less than the pressure exponents of the propellants (TAA-55 and TAR-55).

It was found that the burning rate of the AP particles is little dependent on the addition of the RDX particles; however, it is strongly affected by the type of binder used, as shown in Figs. 8 and 9.

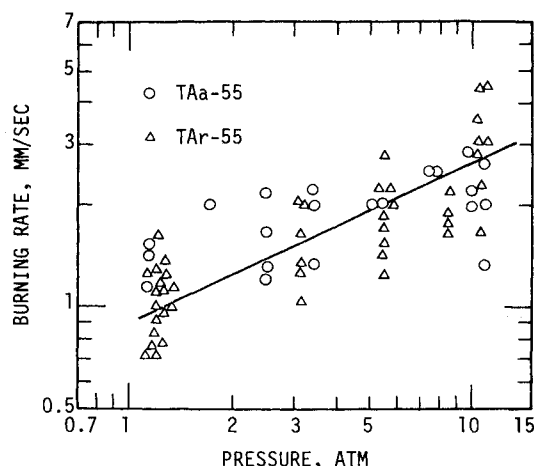


Fig. 9 Burning rate of the AP particles in AP and RDX/AP propellants (HTPE binder) showing little effect of the addition of RDX particles on burning rate.

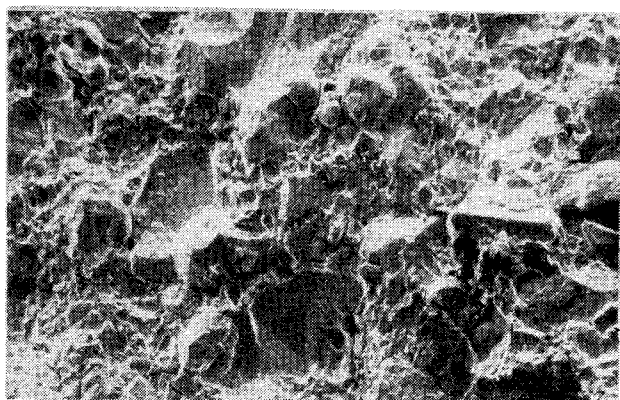


Fig. 10a Scanning electron micrograph of the RDX/AP propellant (HTPB binder) surface before combustion.

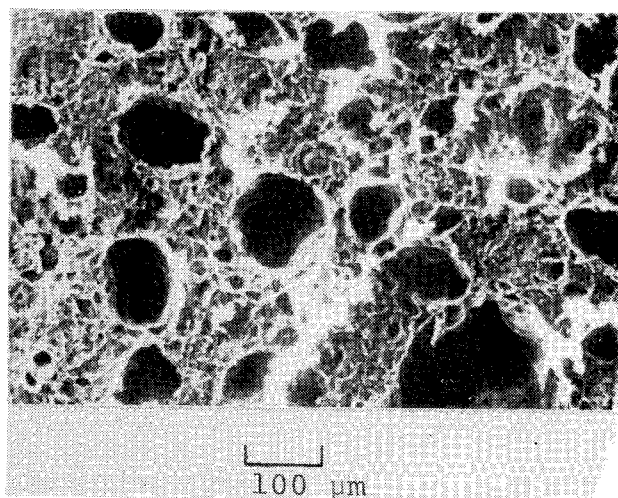


Fig. 10b Scanning electron micrograph of the RDX/AP propellant (HTPB binder) surface after self-extinction.

Burning Surface Structures of RDX/AP Propellants

The burning surface structures of PB-Ra-55 and TAr-55 were observed by high-speed microphotographs during propellant burning at pressures between 2 and 25 atm. The burning surface of PB-Ra-55 was very heterogeneous and irregularly regressing. A large number of flame streams were generated from the burning surface. They were produced by the decom-

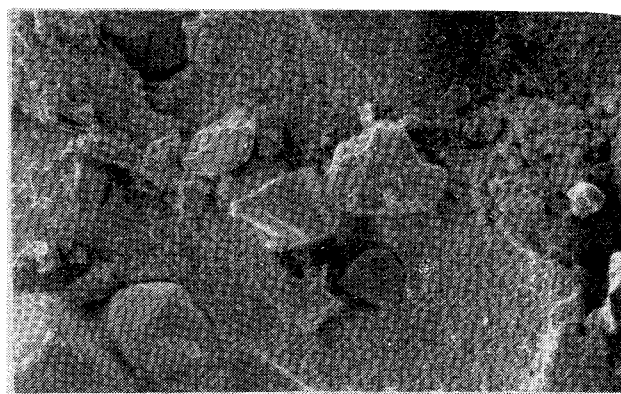


Fig. 11a Scanning electron micrograph of the RDX/AP propellant (HTPE binder) surface before combustion.

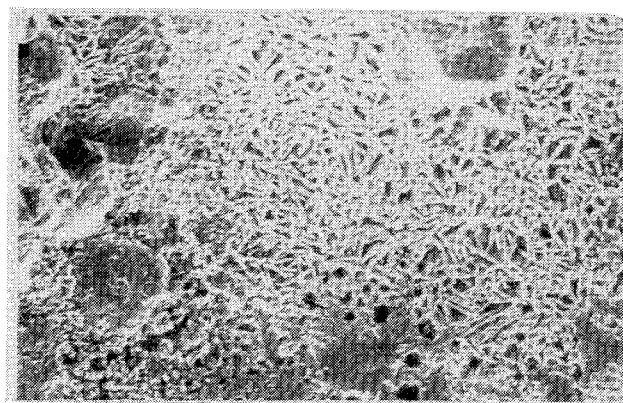


Fig. 11b Scanning electron micrograph of the RDX/AP propellant (HTPE binder) surface after self-extinction.

position gases of the AP particles and the HTPB binder which surrounded each particle. On the other hand, the burning surface of TAr-55 was somewhat different from that of PB-Ra-55. The burning surface of TAr-55 was more homogeneous and was locally melted.

The burning surfaces of propellants that self-extinguished at low pressures were photographed by a scanning electron microscope. As shown in Figs. 10 and 11, there exist a large number of crystalline RDX and AP particles on the burning surfaces of PB-Ra-55 and TAr-55 before burning. However, no crystalline particles were seen on the self-extinguished surface of PB-Ra-55 at 1 atm. A large number of holes are seen, which were produced by the burning of the RDX and AP particles. This result indicates that at low pressure the burning rates of the RDX and AP particles are faster than the decomposition rate of the HTPB binder which surrounds these particles.

On the other hand, the self-extinguished surface of TAr-55 at 1 atm showed a significantly different structure when compared with that of PB-Ra-55. The surface consisted of large-sized crystalline particles and finely divided crystals. The large crystalline particles were determined to be AP particles and the finely divided crystals were recrystallized RDX. It is suspected that the RDX particles mix in the propellant melt and diffuse into the melting HTPE binder, forming an energetic mixture at the burning surface. When self-extinction occurred and the temperature of the burning surface decreased, finely divided RDX was recrystallized from the energetic mixture.

These measurement results show that the role of binder on the burning rate characteristics of RDX/AP propellants is significant, and burning rate models which attempt to predict the burning rate characteristics must take into account the physical and chemical properties of the binder used.

Conclusions

The combustion zone of AP propellants is altered significantly by the addition of RDX particles. The AP particles produce high-temperature flamelets, and the RDX particles produce a low-temperature flame zone above the burning surface. Thus the temperature in the gas phase fluctuates with high amplitudes due to the heterogeneous flame structure produced by the RDX and AP particles.

The measurements of the temperature gradient just above the burning surface revealed that the heat feedback from the gas phase to the burning surface is reduced by the addition of RDX, which, in turn, decreases the burning rate. Examination of the self-extinguished burning surface of the RDX/AP/HTPE propellants shows finely divided recrystallized RDX dispersed on the burning surface and crystalline AP particles. However, neither recrystallized RDX nor crystalline AP particles are seen on the self-extinguished surface when the HTPB binder is used. Thus the role of binder on the burning rate characteristics of RDX/AP propellants appears to be significant.

References

- ¹Hermance, C.E., "A Model of Composite Propellant Combustion Including Surface Heterogeneity and Heat Generation," *AIAA Journal*, Vol. 4, Sept. 1966, pp. 1629-1637.
- ²Lengelle, G., Brulard, J., and Moutet, H., "Combustion Mechanisms of Composite Solid Propellants," *Sixteenth Symposium (International) on Combustion*, The Combustion Institute, Pittsburgh, Pa., 1976, pp. 1257-1269.
- ³King, M., "Model for Steady State Combustion of Unimodal Composite Solid Propellants," AIAA Paper 78-216, 1978.
- ⁴Beckstead, M.W., Derr, R.L., and Price, C.F., "A Model of Composite Solid-Propellant Combustion Based on Multiple Flames," *AIAA Journal*, Vol. 8, Dec. 1970, pp. 2200-2207.
- ⁵Kubota, N., Takizuka, M., and Fukuda, T., "Combustion of Nitramine Composite Propellants," AIAA Paper 81-1582, 1981.
- ⁶McCarty, K.P., Isom, K.B., and Jacox, J.L., "Nitramine Propellant Combustion," AIAA Paper 79-1132, 1979.
- ⁷Kubota, N., "Combustion Mechanism of Nitramine Composite Propellants," *Eighteenth Symposium (International) on Combustion*, The Combustion Institute, Pittsburgh, Pa., 1981, pp. 187-194.
- ⁸Cohen, N.S. and Price, C.F., "Combustion of Nitramine Propellants," *Journal of Spacecraft and Rockets*, Vol. 12, Oct. 1975, pp. 608-612.
- ⁹Kubota, N., Masamoto, T., and Hazama, M., "Combustion of HMX Composite Propellants," *Proceedings of the Twelfth International Symposium on Space Technology and Science*, AGNE Publishing, Inc., Tokyo, 1977, pp. 507-512.
- ¹⁰Zimmer-Galler, R., "Correlations Between Deflagration Characteristics and Surface Properties of Nitramine-Based Propellants," *AIAA Journal*, Vol. 6, Nov. 1968, pp. 2107-2110.
- ¹¹Beckstead, M.W., Derr, R.L., and Price, C.F., "The Combustion of Solid Monopropellants and Composite Propellants," *Thirteenth Symposium (International) on Combustion*, The Combustion Institute, Pittsburgh, Pa., 1971, pp. 1047-1056.
- ¹²Ben-Reuven, M., Caveny, L.H., Vichnevetsky, R.J., and Summerfield, M., "Flame Zone and Sub-surface Reaction Model for Deflagrating RDX," *Sixteenth Symposium (International) on Combustion*, The Combustion Institute, Pittsburgh, Pa., 1976, pp. 1223-1233.
- ¹³Steinz, J.A., Stang, P.L., and Summerfield, M., "The Burning Mechanism of Ammonium Perchlorate-Based Composite Solid Propellants," AIAA Paper No. 68-658, 1968.

From the AIAA Progress in Astronautics and Aeronautics Series

THERMOPHYSICS OF ATMOSPHERIC ENTRY—v. 82

Edited by T.E. Horton, The University of Mississippi

Thermophysics denotes a blend of the classical sciences of heat transfer, fluid mechanics, materials, and electromagnetic theory with the microphysical sciences of solid state, physical optics, and atomic and molecular dynamics. All of these sciences are involved and interconnected in the problem of entry into a planetary atmosphere at spaceflight speeds. At such high speeds, the adjacent atmospheric gas is not only compressed and heated to very high temperatures, but strongly reactive, highly radiative, and electronically conductive as well. At the same time, as a consequence of the intense surface heating, the temperature of the material of the entry vehicle is raised to a degree such that material ablation and chemical reaction become prominent. This volume deals with all of these processes, as they are viewed by the research and engineering community today, not only at the detailed physical and chemical level, but also at the system engineering and design level, for spacecraft intended for entry into the atmosphere of the earth and those of other planets. The twenty-two papers in this volume represent some of the most important recent advances in this field, contributed by highly qualified research scientists and engineers with intimate knowledge of current problems.

544 pp., 6 × 9, illus., \$30.00 Mem., \$45.00 List

TO ORDER WRITE: Publications Order Dept., AIAA, 1633 Broadway, New York, N.Y. 10019